Elevate Series

ORIGINAL RESEARCH

AHNAK2 Promotes the Progression of Pancreatic Ductal Adenocarcinoma by Maintaining the Stability of c-MET

Zhaohui Chen [1,2,]*, Pengbiao Miao[1,3,]*, Hongcao Lin[1,2], Yanan Lu[1,4]

[1]Guangdong Provincial Key Laboratory of Malignant Tumor Epigenetics and Gene Regulation, Sun Yat-sen Memorial Hospital, Sun Yat-sen University, Guangzhou, Guangdong, People's Republic of China; [2]Shenshan Medical Center, Memorial Hospital of Sun Yat-sen University, Shanwei, Guangdong, People's Republic of China; [3]Department of Pancreatobiliary Surgery, Sun Yat-sen Memorial Hospital, Sun Yat-sen University, Guangzhou, Guangdong, People's Republic of China; [4]Department of Anesthesiology, Sun Yat-sen Memorial Hospital, Sun Yat-sen University, Guangzhou, Guangdong, People's Republic of China

*These authors contributed equally to this work

Correspondence: Yanan Lu, Tel +86-020-81332020, Email luynan@mail.sysu.edu.cn

Purpose: Pancreatic ductal adenocarcinoma (PDAC) is extremely malignant and rapidly progresses. The overall response rate of PDAC to current treatment methods is still unsatisfactory. Thus, identifying novel targets and clarifying the underlying mechanisms associated with PDAC progression may potentially offer additional treatment strategies. AHNAK2 is aberrantly expressed in a variety of tumors and exerts pro-tumorigenic effects. However, the biological role of AHNAK2 in PDAC remains poorly understood.
Methods: The expression of AHNAK2 in PDAC and paired non-tumor tissues was detected by immunohistochemistry (IHC) and quantitative real-time polymerase chain reaction (qRT-PCR). Lentivirus knockdown was performed to investigate the impact of AHNAK2 on the biological function of pancreatic cancer cells. The subcutaneous cell-derived xenograft (CDX) model and the KPC spontaneous mouse model with AHNAK2 silencing were used to observe the effects of AHNAK2 on tumor growth and prognosis. The expression of c-MET at protein level in response to HGF treatment was assessed using western blot.
Results: Our results demonstrated that AHNAK2 was highly expressed in PDAC clinical samples and associated with poor prognosis. Knockdown of AHNAK2 significantly inhibited the proliferation, migration, and invasion of pancreatic cancer cells. AHNAK2 knockdown or knockout resulted in tumor growth suppression and prolonged survival in mice with PDAC. In addition, AHNAK2 and c-MET expression levels showed a significant positive correlation at the post-transcriptional level. Mechanistically, AHNAK2 promoted tumor progression by preventing c-MET degradation and persistently activating the HGF/c-MET signaling pathway.
Conclusion: Overall, our study revealed that AHNAK2 plays an important role in PDAC progression by modulating the c-MET signaling pathway, and targeting AHNAK2 may be an effective therapeutic strategy for PDAC.
**Keywords:** pancreatic ductal adenocarcinoma, AHNAK2, c-MET, tumor progression, HGF/c-MET pathway

Introduction

Pancreatic ductal adenocarcinoma (PDAC) is one of the most malignant and lethal types of cancer with a 5-year survival rate of less than 12%.[1] The incidence of PDAC has increased over the years, and mortality remains high mainly due to its aggressiveness and late diagnosis, even with advanced surgical interventions and modern therapeutics.[2] PDAC is a well-defined multistep process with altered histological features during malignant transformation.[3] Clinical and scientific efforts have been made to develop novel treatment approaches for PDAC.[4–7] Thus, exploring potential molecular targets and underlying mechanisms in pancreatic carcinogenesis and tumor progression is urgently needed for the early diagnosis and identification of additional effective treatments for PDAC.

AHNAK nucleoprotein 2 (AHNAK2) is a member of the AHNAK protein family with a molecular weight greater than 600 kDa,[8,9] and its function has been gradually unveiled in recent years. Studies have reported that AHNAK2 is closely associated with oncogenesis in clear cell renal carcinoma,[10] thyroid carcinoma,[11] lung adenocarcinoma,[12] and uveal melanoma.[13] Additionally, AHNAK2 has been reported as a genetic indicator for PDAC diagnosis and

431

Graphical Abstract
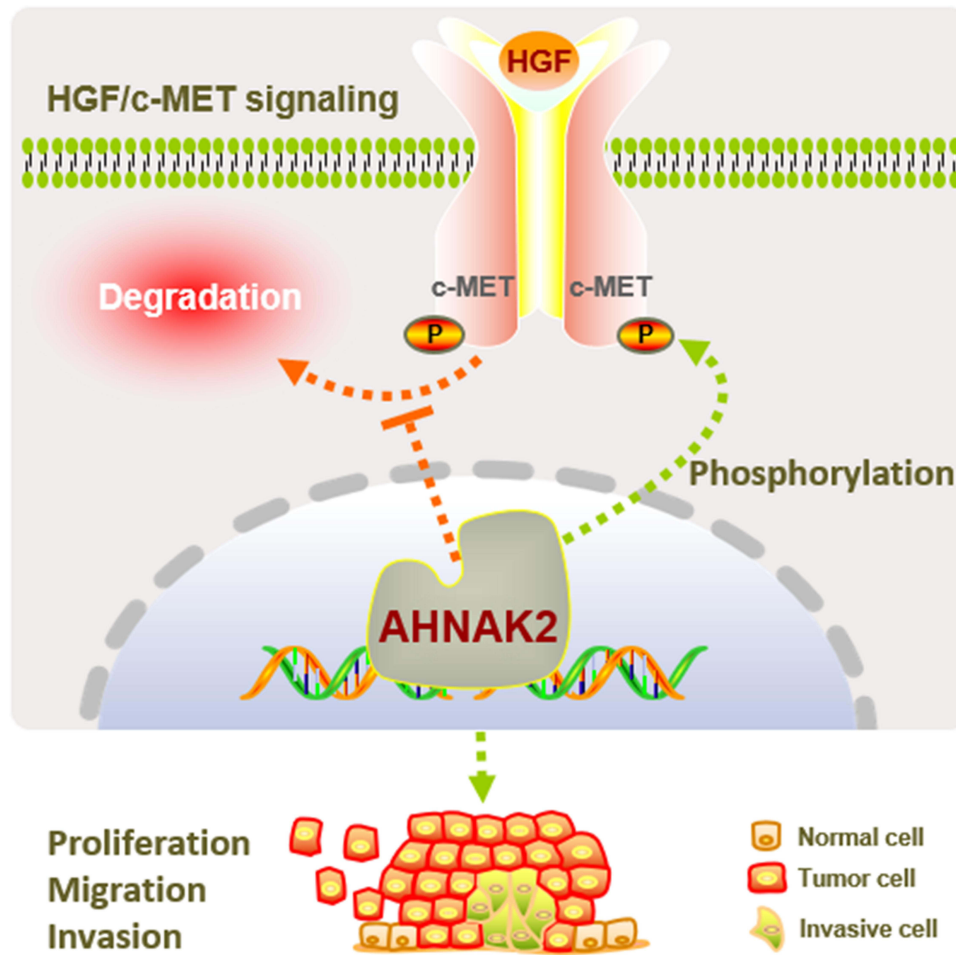
prognosis.[9,14–16] Previous evidence suggests that AHNAK2 may promote tumor proliferation, migration, and survival via HIF-1-mediated epithelial-mesenchymal transition (EMT) in hypoxia[10] and the NF-κB[11] and PI3K/AKT[13] pathways. However, the biological properties of AHNAK2 in PDAC are poorly understood. To date, there is a lack of studies on the biological function of AHNAK2 and its underlying molecular mechanisms in the development and progression of pancreatic cancer. This dearth of studies significantly impedes future exploration of AHNAK2 as a possible therapeutic target for PDAC.

c-MET is a member of the receptor tyrosine kinases (RTKs) that is activated upon binding to the ligand hepatocyte growth factor (HGF) and mediates a variety of biological activities in cancer cells, including proliferation, invasion, and metastasis.[17] Moreover, c-MET signaling plays a crucial role in regulating the process involved in pancreatic tumor progression.[18–20] Elevated c-MET protein levels are directly and positively correlated with human pancreatic tumor staging.[21,22] Studies have revealed that AHNAK proteins could activate various signaling pathways triggered by HGF-c-MET response to favor tumor progression.[11,13,23] Therefore, we sought to explore whether there is an interactive association between AHNAK2 and c-MET in PDAC that promotes tumor progression.

In the present study, we demonstrated that overexpression of AHNAK2 was closely correlated with the malignant phenotype and poor prognosis of PDAC, which was related to the modulation of c-MET stability. Our study confirmed the important role of AHNAK2 in tumor progression, and targeting AHNAK2 might be a therapeutic strategy for the management of patients with PDAC.

Materials and Methods

Database Data Acquisition

Transcriptional expression data of AHNAK2 and corresponding clinical information were downloaded from the official website of The Cancer Genome Atlas Program (TCGA) (https://www.cancer.gov/ccg/research/genome-sequencing/tcga). The RNA-Seq gene expression data, with the workflow type of HTSeq-FPKM, were transformed into TPM format and underwent log2 conversion for further analysis. In the Gene Expression Omnibus (GEO) repository of NCBI, microarray analysis results submitted by worldwide researchers were available. A microarray analysis focusing on AHNAK2 within the GSE15471 dataset, which included data from 36 primary PDAC tumors and their paired adjacent normal tissues, was conducted. Limma package (version: 3.40.2) of R software was employed to study the differential expression of AHNAK2.

Patients and Clinical Samples

Tumor tissues and adjacent non-tumor tissues were collected from 56 patients who had undergone surgery for PDAC at Sun Yat-sen Memorial Hospital, Sun Yat-sen University, from June 2013 to August 2017. The diagnoses of PDAC and surgical specimens were confirmed by two independent professional pathologists. The studies involving human participants were reviewed and approved by the Ethics Committee of Sun Yat-sen Memorial Hospital (Ethics No.SYSKY-2023-735-01). Written informed consent was obtained from all the patients. All methods related to the patients in this study were performed in accordance with the principles stated in the Declaration of Helsinki. The detailed clinical characteristics of the patients were displayed in Supplementary Table 1.

Cell Lines and Culture

The human pancreatic cancer cell lines PANC-1, AsPC-1, CFPAC-1, MIA PaCa-2, Capan-2, BxPC-3, SW1990, and the human pancreatic duct epithelial cell line (hTERT-HPNE) were purchased from the American Type Culture Collection (ATCC, Rockville, MD, USA). PANC-1, MIA PaCa-2, SW1990, Capan-2 and hTERT-HPNE were cultured in Dulbecco's Modified Eagle's medium (DMEM, BI, Israel); AsPC-1 and BxPC-3 were cultured in RPMI-1640 medium (BI, Israel). All culture medium were supplemented with 10% fetal bovine serum (Gibco, Thermo Fisher Scientific, USA) and 1% penicillin/streptomycin, and cells were cultured at 37 °C in humidified air with 5% CO_2. Information on lentiviral transduction and plasmid transfection was included in Supplementary Methods 1 and 2.

In vitro Biological Function Experiments

A comprehensive description of the CCK-8 assay, colony formation assay, transwell invasion assay, and wound healing assay was displayed in Supplementary Methods 3–6.

Animal Models and Experiments

The animal study was approved by the Animal Experimental Research Ethics Committee of South China University of Technology (Ethics No.2022-059) and performed in accordance with the NIH guidelines for the care and use of laboratory animals (8th edition, NIH).

Subcutaneous cell-derived xenograft (CDX) BALB/c nude mice aged 4–6 weeks were purchased and housed at the Laboratory Animal Center of South China University of Technology in a pathogen-free environment. Necessary measures were taken to minimize the suffering of the mice. Briefly, 1×10^7 PANC-1 cells stably transfected with shCtrl or shAHNAK2 were suspended in 100 μL serum-free DMEM and injected subcutaneously into the right flank of BALB/c nude mice as previously described.[24] Tumor volume was measured at 3-day intervals and calculated using the following formula: volume = length $\times$ width^2/2. Mice were euthanized on day 30 after cell inoculation, and tumor tissues were fixed with 4% paraformaldehyde, followed by paraffin embedding for IHC assay or frozen in liquid nitrogen for further investigation.

The AHNAK2 knockout mouse models LSL-Kras$^{G12D/+}$, LSL-Trp53$^{R172H/+}$ (129S4-Trp53tm2Tyj/J), AHNAK2$^{-/-}$, and Pdx1-Cre mouse strains (C57BL/6J background) were used to generate the AHNAK2 knockout mouse model.[25,26]

First, these strains were intercrossed to generate the genotypes of LSL-Kras$^{G12D/+}$-Trp53$^{R172H/+}$ (KP) and AHNAK2$^{-/-}$-Pdx1-Cre (AHC). KP mice were then crossed with AHC mice to obtain the experimental groups: LSL-Kras$^{G12D/+}$-LSL-Trp53$^{R172H/+}$-Pdx1-Cre (KPC) and LSL-Kras$^{G12D/+}$-LSL-Trp53$^{R172H/+}$-Pdx1-Cre/+ -AHNAK2$^{-/-}$ (AHNAK2$^{-/-}$KPC). All genotypes of mice were purchased from Shanghai Model Organisms.

RNA Isolation and Quantitative Real-Time PCR (qRT–PCR)

Total RNA of tissue and cell samples was isolated using RNAiso Plus (TaKaRa Bio, Japan) according to the manufacturer's instructions and reverse-transcribed to cDNA using PrimeScript^{TM} RT Master Mix (TaKaRa Bio, Japan). qRT-PCR was performed with the Light Cycler 480 detection system (Roche, Basel, Switzerland) under the instructions of the TB Green$^®$Premix ExTaqTM kit (TaKaRa Bio, Japan). GAPDH was used as an internal control. Relative gene expression levels in cells or tissues were calculate with the standardized method of $2^{-\Delta\Delta CT}$. All the primers used were listed in Supplementary Table 2.

Immunohistochemistry (IHC) and Immunofluorescence (IF)

Complete descriptions for immunohistochemistry and immunofluorescence are provided in Supplementary Methods 7 and 8.

Western Blotting

Cells were harvested and lysed on ice in RIPA lysis buffer (CWBIO, China) containing protease and phosphatase inhibitors (CWBIO, China), followed by centrifugation at 14,000 rpm for 15 min at 4 °C. Bicinchoninic acid (BCA) protein assay kit (CWBIO, China) was used to quantify protein concentrations. Proteins from each sample were separated by SDS-PAGE gels, transferred to PVDF membranes, and then blocked with 5% BSA. The membranes were incubated overnight at 4°C with primary antibodies including AHNAK2 (1:1000, Proteintech, #17682-1-AP), c-MET (1:1000, #ab216574, Abcam), p-MET (Tyr1234/1235) (1:1000, #3077S, CST), Akt (1:1000, #4691, CST), p-Akt (Ser473) (1:2000, #4060, CST) and GAPDH (1:10,000, #ab181602, Abcam). The protein strips were then washed three times with 1×TBST and incubated with HRP-conjugated secondary antibodies at room temperature for an hour. Bands were detected with ECL detection system (Millipore, Germany) and captured using SmartChemi 910 plus (Sage, Beijing).

Statistical Analysis

Statistical analysis was performed using SPSS version 12.0 (IBM Corp, USA). The Student's *t*-test was used for comparisons between the two groups. One-way analysis of variance (ANOVA) with Bonferroni's test was used for multiple comparisons. Survival data were plotted according to the Kaplan-Meier method and analyzed using a Log rank test. Correlation analyses were performed using Spearman correlation test. All experiments were conducted at least three times, and the data were presented as mean ± SD. $p < 0.05$ was considered as statistically significant.

Results
AHNAK2 Expression in Clinical Samples and the Cancer Cell Lines of PDAC

To identify the specific role of AHNAK2 in PDAC, we first examined through immunohistochemistry (IHC) in normal non-tumor adjacent tissues and PDAC specimens. Compared to normal tissues, high expression of AHNAK2 was found in PDAC (Figure 1A). More representative images from PDAC patients with high expression of AHNAK2 were available in Supplementary Figure 1. To verify the gene expression of AHNAK2 in PDAC, we analyzed tumour samples and adjacent non-tumour tissues from recruited PDAC patients by qRT-PCR. Our data showed that the mRNA expression of AHNAK2 in PDAC tissues was significantly higher than that in paired adjacent normal tissues (Figure 1B). Next, the mRNA expression of AHNAK2 was assessed in a variety of human pancreatic cancer cell lines (Figure 1C), and PANC-1 was selected for subsequent experiments because of its highest relative expression in comparison to human normal pancreatic ductal cells (hTERT-HPNE). Immunofluorescence (IF) was employed to evaluate the protein expression of AHNAK2. The IF results also indicated that AHNAK2 was highly expressed in PANC-1 cells (Figure 1D). These findings were further validated in the mRNA expression profile of AHNAK2 by microarray analysis of PDAC tumor
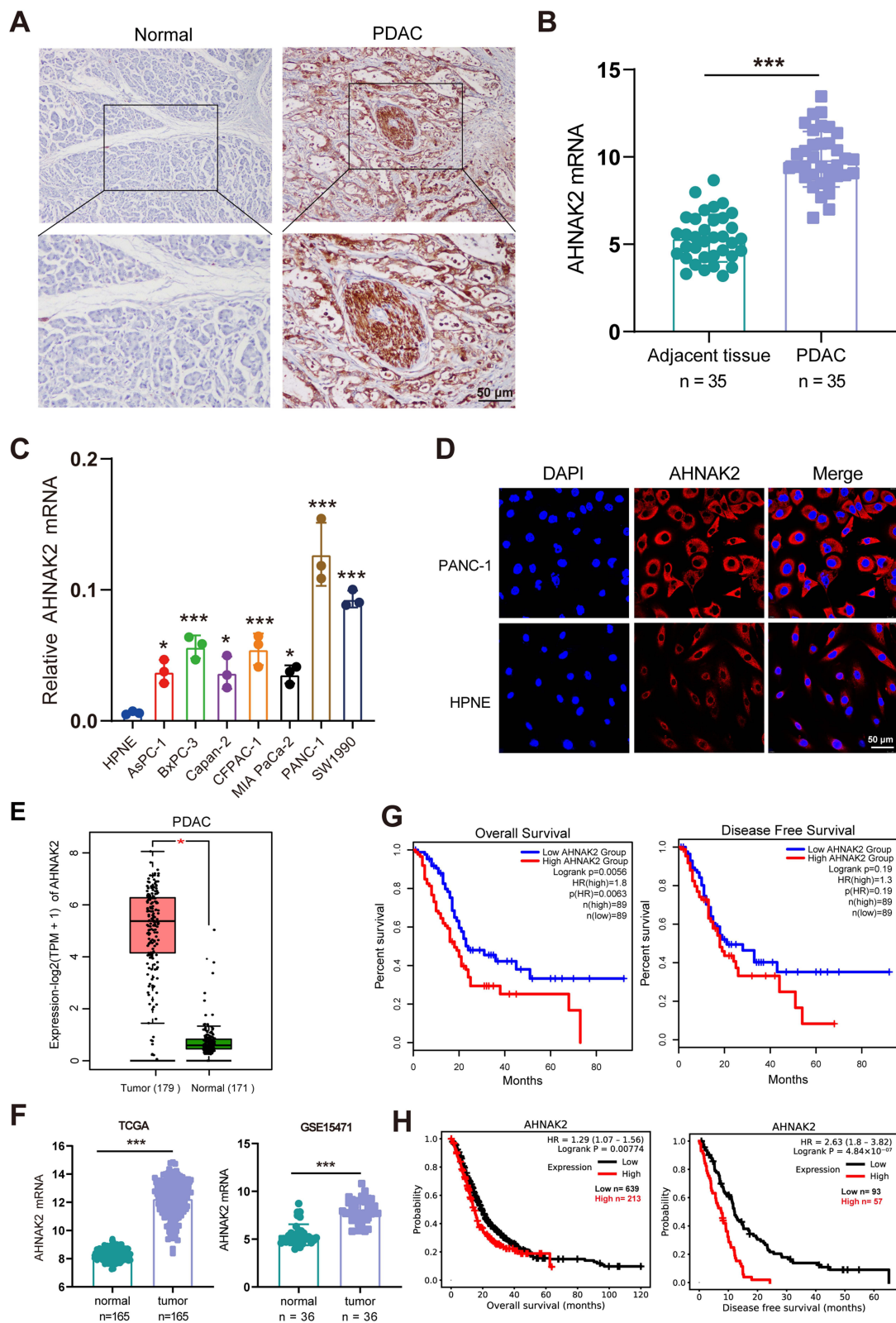
Figure 1 AHNAK2 is highly expressed in PDAC and pancreatic cancer cell line. (**A**) Representative images of AHNAK2 immunohistochemical staining in normal non-tumor adjacent tissues and pancreatic ductal adenocarcinoma (PDAC) (scale bar, 50 μm). (**B** and **C**) qRT-PCR analysis of AHNAK2 mRNA in PDAC samples, non-tumor adjacent tissues (n=35), and pancreatic cancer cell line (n=3). (**D**) Representative images of AHNAK2 immunofluorescence staining in PANC-1 and hTERT-HPNE cells (scale bar, 50 μm). (**E**) The mRNA levels of AHNAK2 in normal tissues and PDAC tissues from The Cancer Genome Atlas (TCGA) and GTEx databases. (**F**) AHNAK2 mRNA levels by microarray analysis of PDAC samples and non-tumor normal tissues from TCGA and GEO (GSE15471) databases. The expression level of AHNAK2 was significantly positively correlated with both the overall survival (OS) and disease-free survival (DFS) of PDAC patients from TCGA and GTEx (**G**) and Kaplan-Meier plot database (**H**). Each bar represents Mean ± SD. *p<0.05, ***p<0.001.

samples and non-tumor normal tissues from the GEPIA (Figure 1E), TCGA, and GEO (GSE15471) (Figure 1F) databases. The application of survival analysis in GEPIA (http://gepia2.cancer-pku.cn/) (Figure 1G) and Kaplan-Meier plotter (https://kmplot.com) (Figure 1H) datasets indicated that high AHNAK2 expression was associated with shorter disease-free survival overall survival (OS) and disease-free survival (DFS) in patients with PDAC, suggesting that AHNAK2 could serve as an unfavorable prognostic marker.

AHNAK2 Knockdown Inhibits Proliferation, Invasion, and Migration

To analyze the function of AHNAK2, AHNAK2 was silenced using short hairpin RNA (shRNA) in PANC-1 cells. The knockdown efficiency of AHNAK2 was evaluated at both the mRNA and protein levels using qRT-PCR (Figure 2A), Western blot (Figure 2B) and immunofluorescence (Figure 2C), respectively. CCK-8 proliferation assay and colony formation assay were used to assess the proliferation potential of cancer cells. The results showed that impaired AHNAK2 expression suppressed cell proliferation (Figure 2D and E). Wound healing and transwell invasion assay were performed to simulate the horizontal and vertical migration of cancer cells. AHNAK2 knockdown resulted in a significant reduction in invading (Figure 2F) and migrating (Figure 2G) capabilities of cancer cells across the matrigel layer. Taken together, AHNAK2 plays an important role in proliferation, invasion and migration of pancreatic cancer cells.

AHNAK2 Knockdown Reduces Tumor Growth in a CDX Mouse Model

To further explore the in vivo function of AHNAK2, PANC-1 cells stably transfected with either shControl (shCtrl) or shAHNAK2#1 and shAHNAK2#2 were subcutaneously inoculated into BALB/c nude mice to establish a CDX mouse model. Tumor growth in mice transplanted with shAHNAK2 was significantly inhibited (Figure 3A, Supplementary Figure 2), and the tumor volume showed marked regression 18 days post-inoculation (Figure 3B). Consistently, the percentage of Ki67-positive cells was decreased in the shAHNAK2 group, confirming the impaired proliferative ability caused by AHNAK2 knockdown (Figure 3C). These results indicate that a decrease in the expression of AHNAK2 significantly hampers tumor development and proliferation.

Knockout AHNAK2 Impairs Tumorigenicity and Progression in a KPC Mouse Model

Subsequently, to investigate the role of AHNAK2 in pancreatic carcinogenesis and tumor progression, a conditional AHNAK2 knockout (KO) mouse model (KPC$^{AHNAK2-/-}$) was generated as described above. Compared to wild-type (WT) mice, higher protein and mRNA expression levels of AHNAK2 were detected in KPC mice (Figure 4A and B). The average survival time was significantly prolonged following AHNAK2 KO, with a median survival of 200 days compared to 117 days in KPC mice (Figure 4C). In addition, there was a statistically significant difference in the calculated number of mice surviving for more than 120 days in the AHNAK2 KO group compared to the KPC group (Figure 4D). Additionally, Ki67 staining scores were significantly reduced in KPC$^{AHNAK2-/-}$ mice (Figure 4E), confirming that AHNAK2 knockout leads to decreased tumor proliferation and progression. These results demonstrate that AHNAK2 has a strong impact on tumorigenesis and tumor progression.

AHNAK2 Expression is Positively Correlated with c-MET and Regulates c-MET at the Post-Transcriptional Level

c-MET was reported to be overexpressed and contributed to the progression of numerous cancer types, including PDAC. Online correlation analysis of public databases revealed a significant positive correlation between AHNAK2 and c-MET (Figure 5A). We also found an increase in c-MET mRNA level in line with AHNAK2 upregulation in KPC transgenic mice compared to WT mice (Figure 5B). However, no significant changes were observed in the mRNA expression of c-MET following AHNAK2 knockdown or knockout in either transgenic mouse models (Figure 5C) or CDX (Supplementary Figure 3A). In addition, Spearman correlation analysis showed a positive correlation between AHNAK2 and c-MET mRNA in KPC mice (Figure 5D), but not in KPC$^{AHNAK2-/-}$ mice (Figure 5E). Interestingly,
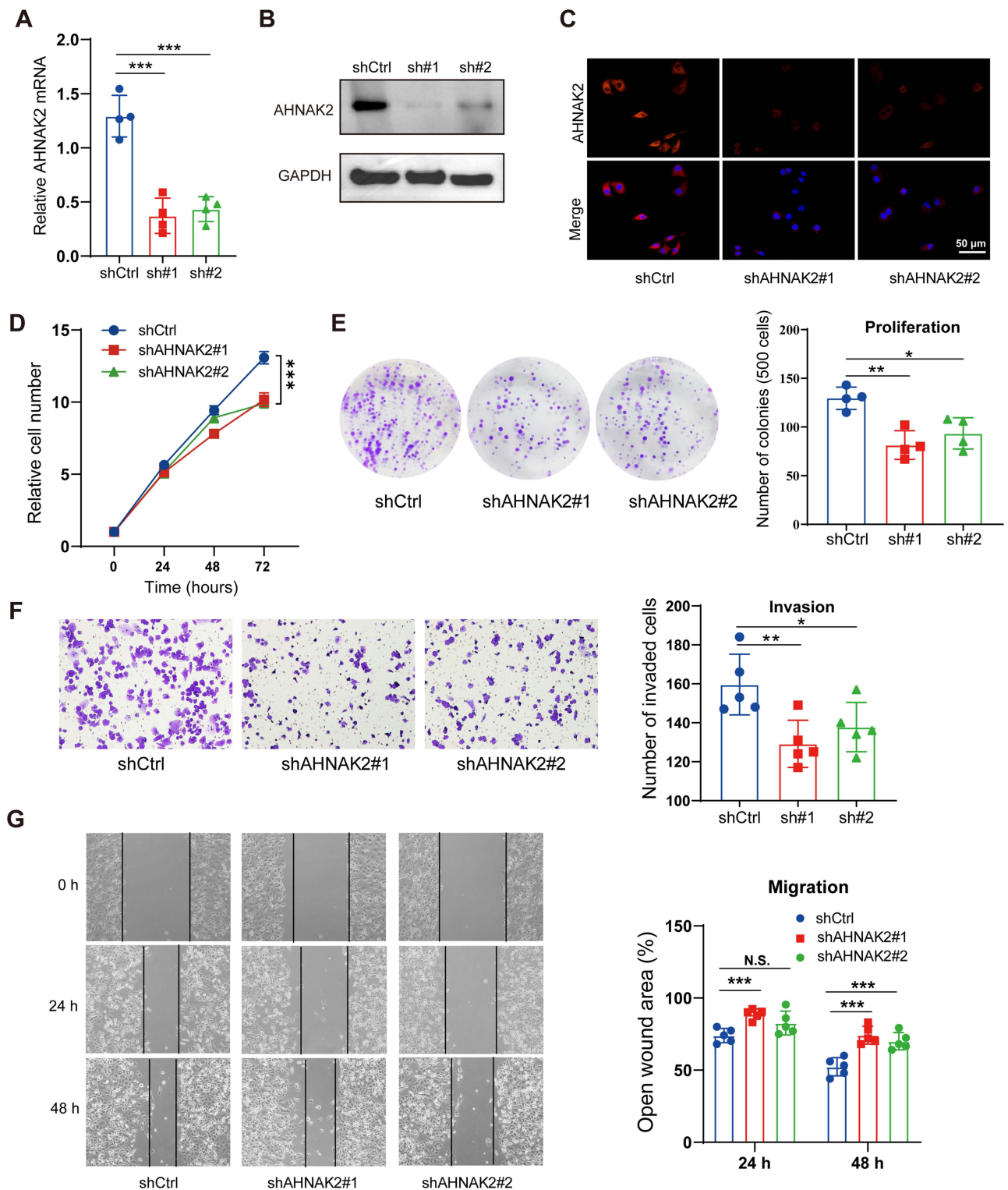
Figure 2 AHNAK2 knockdown inhibits proliferation, invasion, and migration in vitro. The expression levels of AHNAK2 in PANC-1 cells stably transfected with shRNA was analyzed by qRT-PCR (**A**), Western blot (**B**) and immunofluorescence staining (**C**). (**D**) Cell proliferation assay of shControl and AHNAK2 knockdown PANC-1 cells. The relative cell numbers on day 0 were arbitrarily set to 1 (n=5; only comparisons at 72h are shown). (**E**) Colony formation assay in shControl and AHNAK2 knockdown PANC-1 cells. (n=4). Silencing of AHNAK2 in PANC-1 cells significantly reduced their ability to invade in transwell assays (**F**) and migrate in wound healing assays (**G**) (n=5). Each bar represents Mean ± SD. *p<0.05; **p<0.01; ***p<0.001.
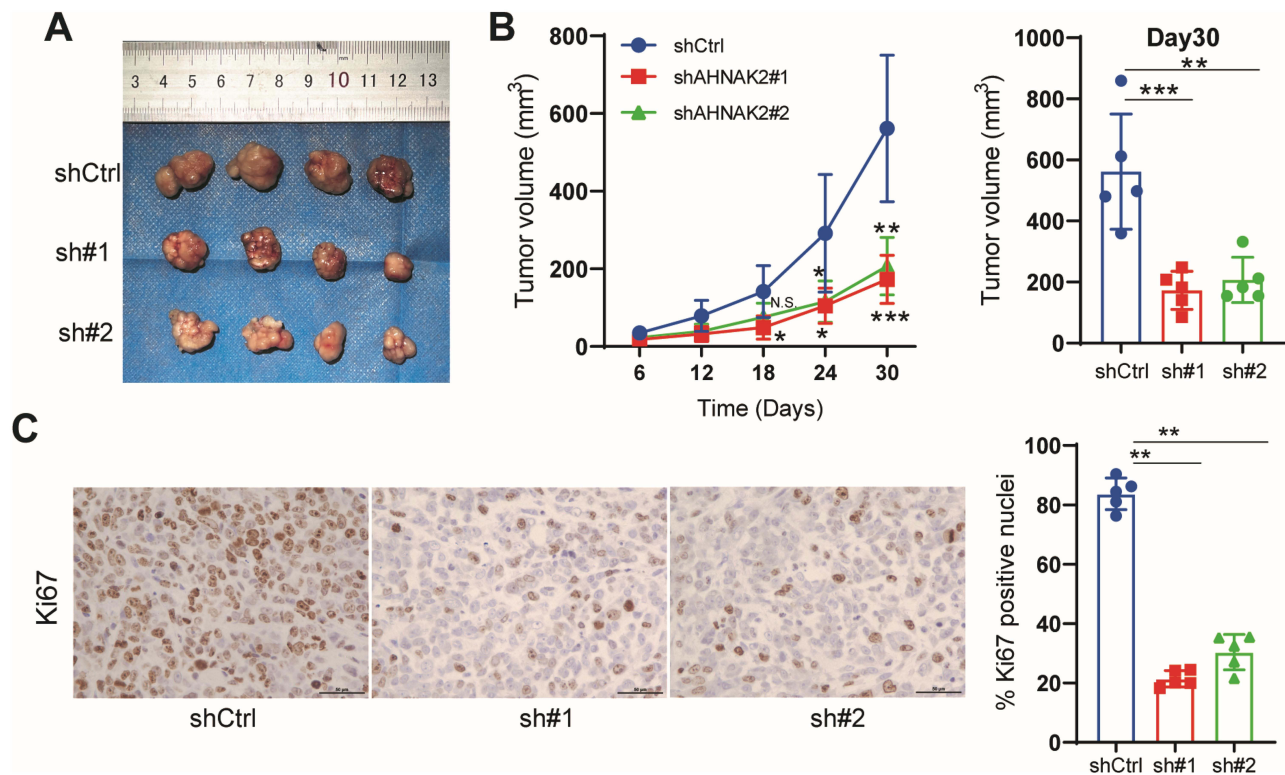**Abbreviation**: N.S., not significant.

Figure 3 AHNAK2 promotes tumor growth and proliferation in CDX models. (**A**) Representative images of xenografts derived from PANC-1 cells stably transfected with shControl and shAHNAK2 groups. (**B**) After subcutaneous injection of shControl and AHNAK2 knockdown cells in mice, tumor growth curves were calculated at an interval of 6 days, showing that the growth of the shAHNAK2 group was inhibited. (**C**) Representative images of immunohistochemical staining of the proliferation marker Ki67 in the excised subcutaneous tumours (scale bar, 50 μm), and quantification of the percentage of Ki67 positive nuclei (n=5). Each bar represents Mean ± SD. *p<0.05; **p<0.01; ***p<0.001.
Abbreviation: N.S., not significant.

the protein expression of c-MET was significantly decreased in KPC$^{AHNAK2-/-}$ mice (Figure 5F) and shAHNAK2 subcutaneous xenograft tumor tissues compared to that in the control groups (Supplementary Figure 3B).

In order to examine the expression profiles of AHNAK2 and c-MET, patients diagnosed with pancreatic adenocarcinoma were categorized into two groups: AHNAK2^{High} and AHNAK2^{Low}, based on the H-score of AHNAK2 identified using IHC. A significant upregulation of c-MET in the AHNAK2^{High} group was observed when compared with the AHNAK2^{Low} groups (Figure 6A and B). The correlation analysis further demonstrated a positive correlation between the H-scores of AHNAK2 and c-MET in PDAC samples (Figure 6C).

These results indicated that AHNAK2 was able to influence the accumulation of the c-MET at the protein level, whereas no significant alteration was detected in the mRNA expression of c-MET, implying that AHNAK2 may have a role in regulating c-MET post-transcriptionally.

AHNAK2 Protects c-MET from Degradation

To ascertain the functional role of AHNAK2 in the c-MET signaling pathway, we analyzed c-MET expression in PANC-1 cell lines transfected with either shCtrl or shAHNAK2 (Original Western blot images are showed in Supplementary Figure 4). The results showed that the reduction of AHNAK2 under knockdown condition led to a decrease in c-MET protein levels (Figure 7A) while mRNA levels remained unaffected (Figure 7B). To determine whether this effect was due to suppressed protein synthesis or increased protein degradation, the cycloheximide (CHX) assay was employed to quantify the half-life of the c-MET protein. The results showed that the half-life of c-MET was significantly reduced after AHNAK2 silencing, indicating a potential role of AHNAK2 in modulating c-MET protein stability (Figure 7C). In addition, the accumulation of c-MET is subject to stimulus-dependent endocytosis induced by HGF treatment, intracellular trafficking, and biodegradation. HGF-dependent c-MET degradation was accelerated after AHNAK2 silencing
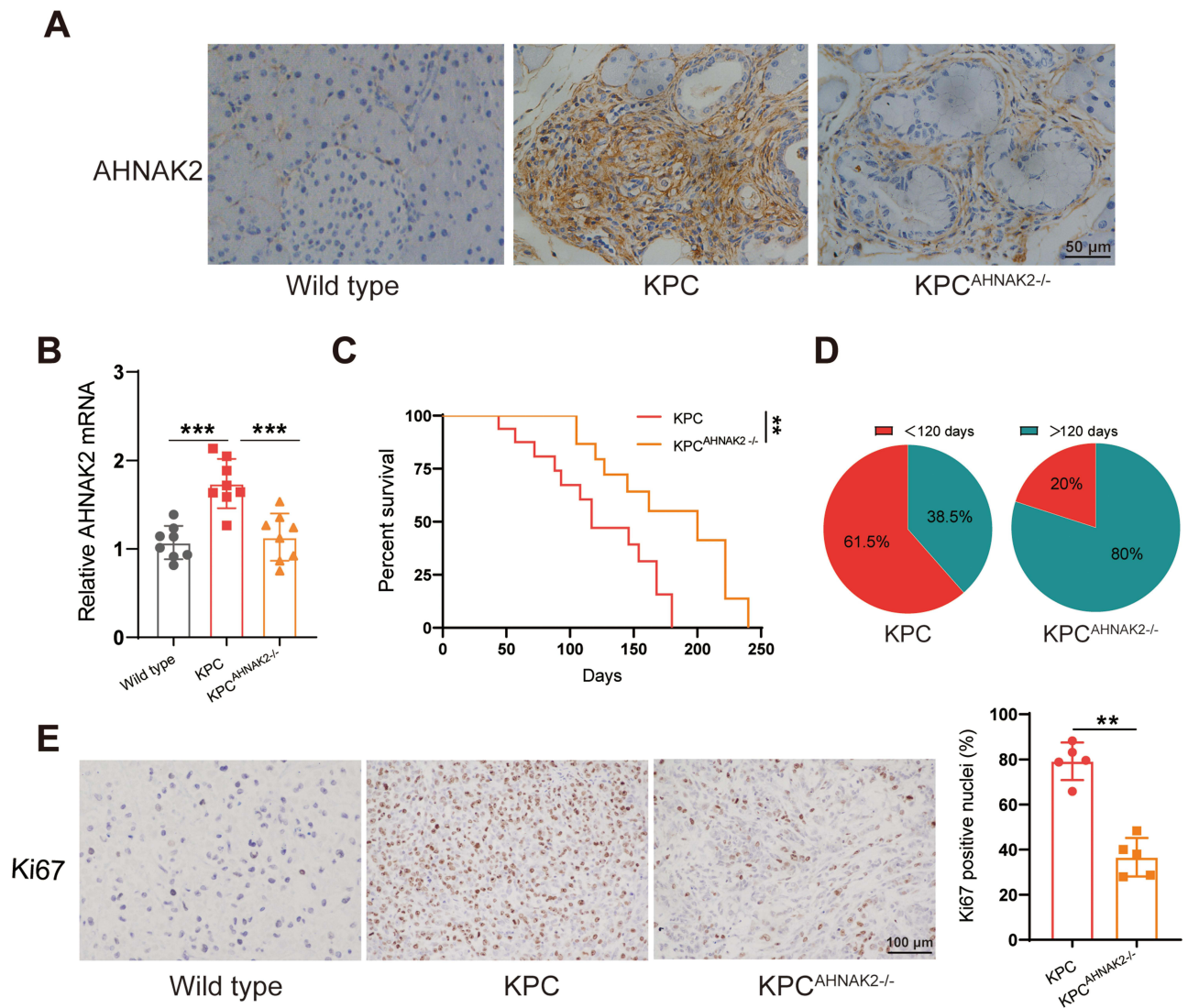
A

B　　**C**　　**D**

E

Figure 4 AHNAK2 knockout impairs tumorigenicity and progression in KPC mice. (**A**) Representative images of AHNAK2 immunohistochemical staining in the pancreas of wild type (WT), KPC and KPC[AHNAK2−/−] mice (scale bar, 50 μm). (**B**) qRT-PCR analysis of AHNAK2 mRNA expression in WT, KPC and KPC[AHNAK2−/−] mice (n=8). (**C**) Kaplan-Meier survival curves of KPC (n=13) and KPC[AHNAK2−/−] mice (n=10). (**D**) Pie charts represent the percentage of animals in each group that survived longer than 120 days (dark green). (**E**) Representative images of immunohistochemical staining of the proliferation marker Ki67 in the pancreatic tissues of WT, KPC and KPC[AHNAK2−/−] mice, and quantification of the nuclei positive for this marker (n=5 per genotype). Each bar represents Mean ± SD. **p<0.01; ***p<0.001.

compared to shCtrl (Figure 7D), which was rescued by the proteasome inhibitor MG-132 (Figure 7E). Moreover, the degradation of c-MET was AHNAK2-specific, since the rescue of AHNAK2 expression by adding the shRNA-resistant form of AHNAK2 partially restored c-MET expression levels (Figure 7F). Furthermore, the expression of p-MET and the p-MET/c-MET ratio following HGF treatment were evaluated (Figure 7D). This revealed a negative regulatory role for AHNAK2 silencing in HGF/c-MET pathway activation, probably by influencing c-MET accumulation and stability.

Discussion

PDAC is a highly malignant tumor that affects the digestive tract and is associated with a poor prognosis. Despite considerable improvements in therapeutic options over the past decades, pancreatic adenocarcinoma remains largely incurable due to difficulties in early diagnosis and lack of effective targets.[27] Therefore, identifying functional and effective targets for halting the malignant progression of PDAC is crucial.

AHNAK2, a large protein featuring a conserved PDZ (PSD-95/Discs-large/ZO-1) domain capable of binding to the C-terminus or docking with specific sequences of target proteins, has recently been implicated as an oncogene involved
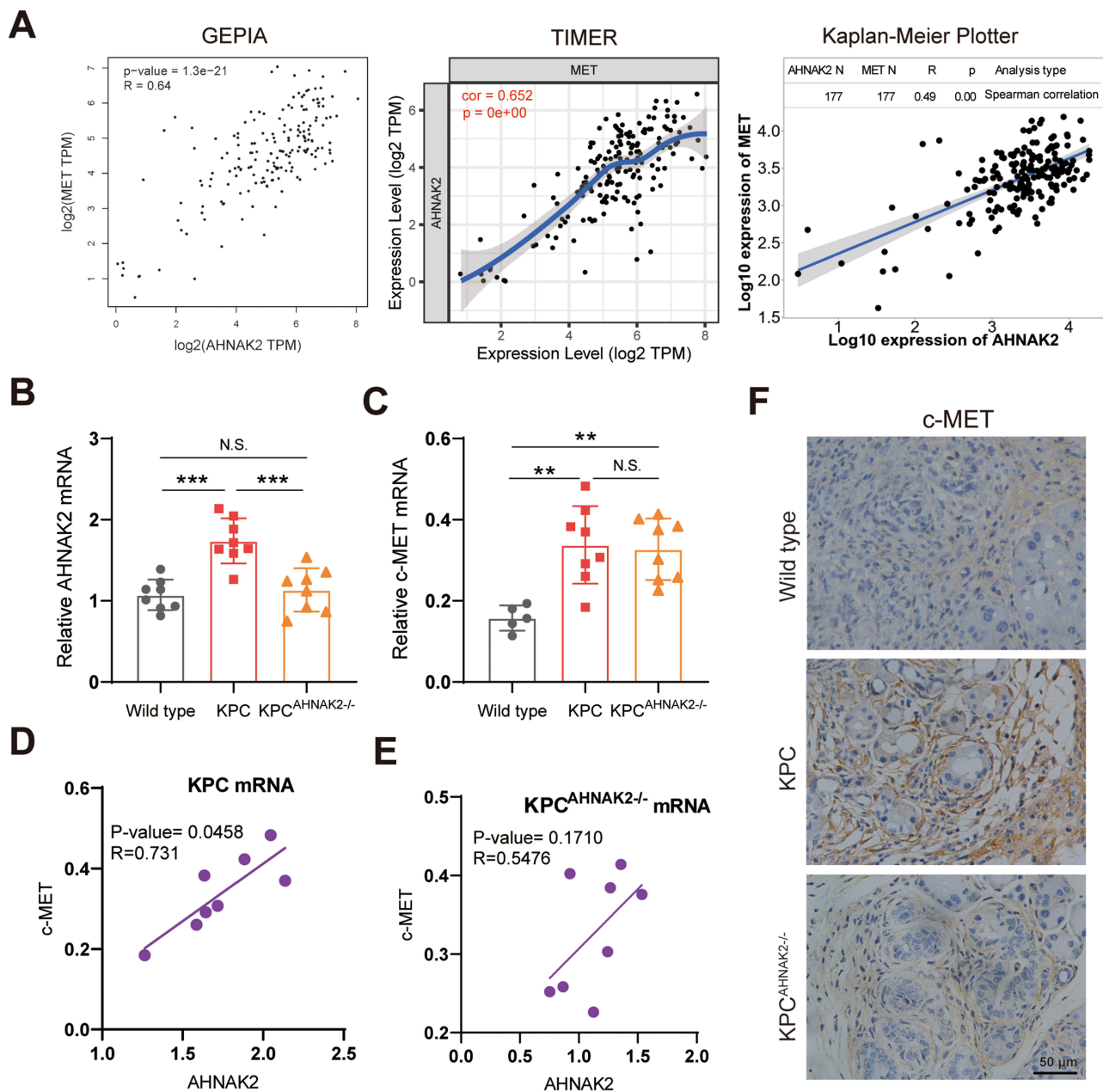
Figure 5 AHNAK2 expression is positively correlated with c-MET expression. (**A**) Correlation analysis of AHNAK2 and c-MET gene expression from GEPIA, Timer and Kaplan-Meier Plotter databases. (**B**) qRT-PCR analysis of AHNAK2 and c-MET mRNA expression in KPC (**B**) and KPC^AHNAK2−/− mice (**C**). The mRNA levels of AHNAK2 and c-MET in KPC mice (**D**) and KPC^AHNAK2−/− mice (**E**) are plotted for correlation analysis (n=8; Spearman correlation test). (**F**) Representative images of c-MET immunohistochemical staining in the pancreas tissue of WT, KPC and KPC^AHNAK2−/− mice (scale bar, 50 μm). Each bar represents Mean ± SD. **p<0.01, p***<0.001.
Abbreviation: N.S., not significant.

in tumor progression.[9] Previous studies have revealed that AHNAK2 is associated with various cellular processes in cancer cells, such as proliferation, migration, and EMT.[10–13] However, only a few studies have investigated the molecular function of AHNAK2 in PDAC. Consistent with previous studies, our study also found that AHNAK2 was highly expressed in PDAC tissues and pancreatic cancer cell lines. Importantly, our findings revealed that AHNAK2 knockdown had detrimental effects on proliferation, migration, and invasion of PANC-1 cells. In agreement with these in vitro results, AHNAK2 silencing effectively diminished tumor growth in CDX mouse models. Notably, the biallelic deletion of AHNAK2 attenuated tumor progression and prolonged the survival of KPC transgenic mice. To our knowledge, this is
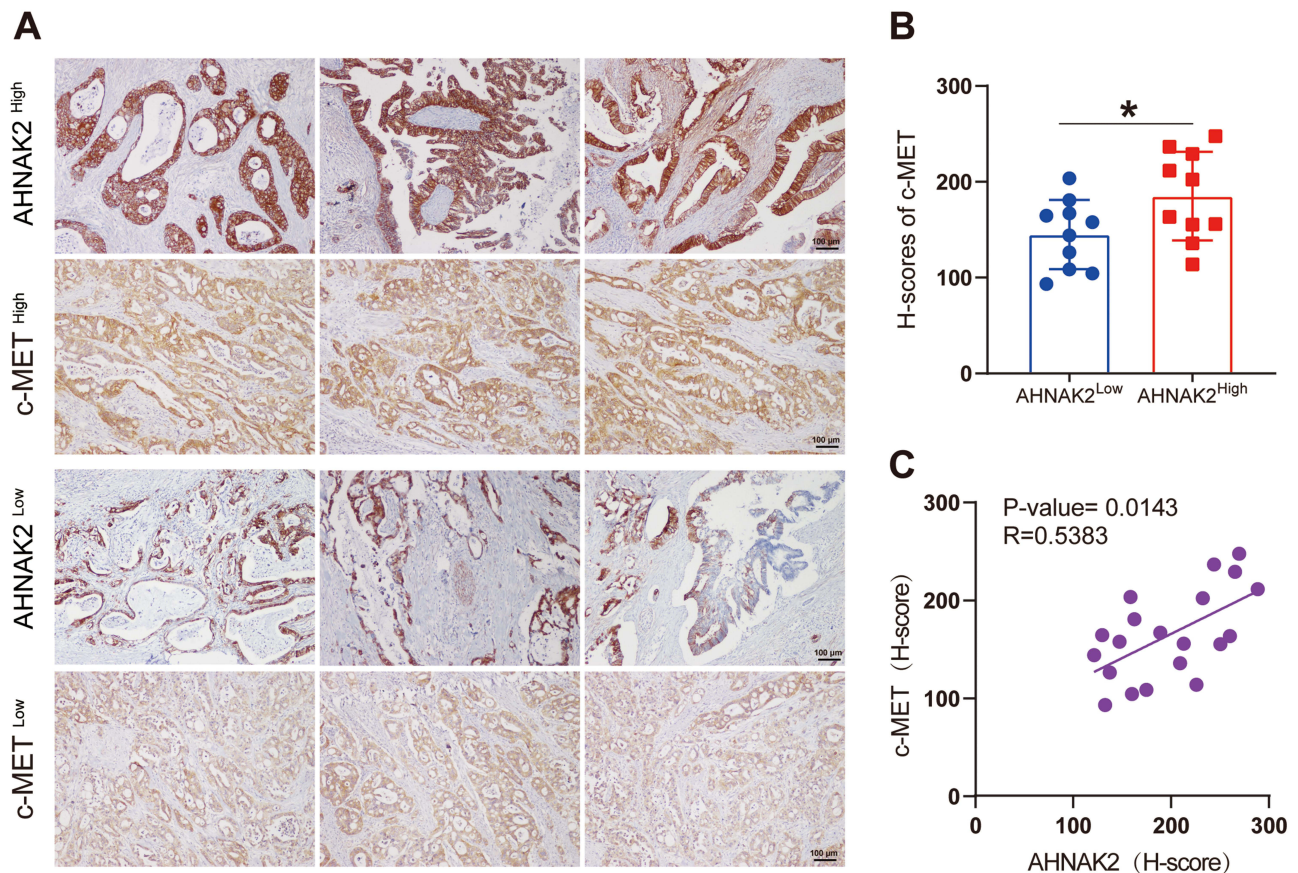
Figure 6 AHNAK2 correlates with c-MET expression in PDAC at protein level. (**A**) Representative immunohistochemical staining images of c-MET expression corresponding to high and low expression of AHNAK2 (AHNAK2[High] and AHNAK2[Low]) in PDAC specimens (n=10). (Scale bar, 100 μm). (**B**) Tumour samples were categorised according to AHNAK2 expression levels into high and low, according to the H-score, and rescored for c-MET. (**C**) Correlation analysis using the H-scores of AHNAK2 and c-MET (Spearman correlation test). Each bar represents Mean ± SD. *p<0.05.

the first study to analyze the molecular function of AHNAK2 using CDX and KPC transgenic mouse models, unmasking the critical role of AHNAK2 in pancreatic carcinogenesis and tumor progression.

The c-MET signaling pathway is generally activated by its native ligand HGF, leading to receptor dimerization and phosphorylation of Tyr^{1234} and Tyr^{1235} within the kinase catalytic domains.[28] In the physiological state, the HGF/c-MET signaling pathway is tightly controlled by multiple regulatory mechanisms to prevent aberrant activation.[29] In fact, HGF/c-MET signaling has been shown to stimulate the growth and progression of pancreatic cancer cells and promote the proliferation, invasion, and metastasis of cancer cells through the activation of several signaling pathways, such as PI3K/Akt, MAPK/ERK, and NF-Kb.[30–32] Interestingly, AHNAK2 had the ability to activate the signaling pathway triggered by HGF-c-MET response to promote tumor progression.[11,13,23] Therefore, we hypothesized and subsequently confirmed the potential involvement of AHNAK2 in the regulation of PDAC via the c-MET signaling pathway. Consistent with the findings from online public databases, our study revealed a substantial positive correlation between the mRNA expression levels of c-MET and AHNAK2 in KPC transgenic mice. However, AHNAK2 knockout or knockdown dramatically decreased c-MET at the protein level, but not at the mRNA level, implying that AHNAK2 may regulate the accumulation of c-MET at the post-transcriptional level.

The regulation of c-MET involves many complicated processes, with different effects depending on the cellular environment.[33,34] Our findings indicate that AHNAK2 may play a role in regulating c-MET at the post-transcriptional level, perhaps leading to the preservation of c-MET stability. It has been demonstrated that the c-MET receptor could be stabilized by DYRK1A in PDAC, contributing to the prolonged activation of extracellular signal-regulated kinase signaling.[35] The findings from our in vitro experiments support the hypothesis that AHNAK2 increases c-MET
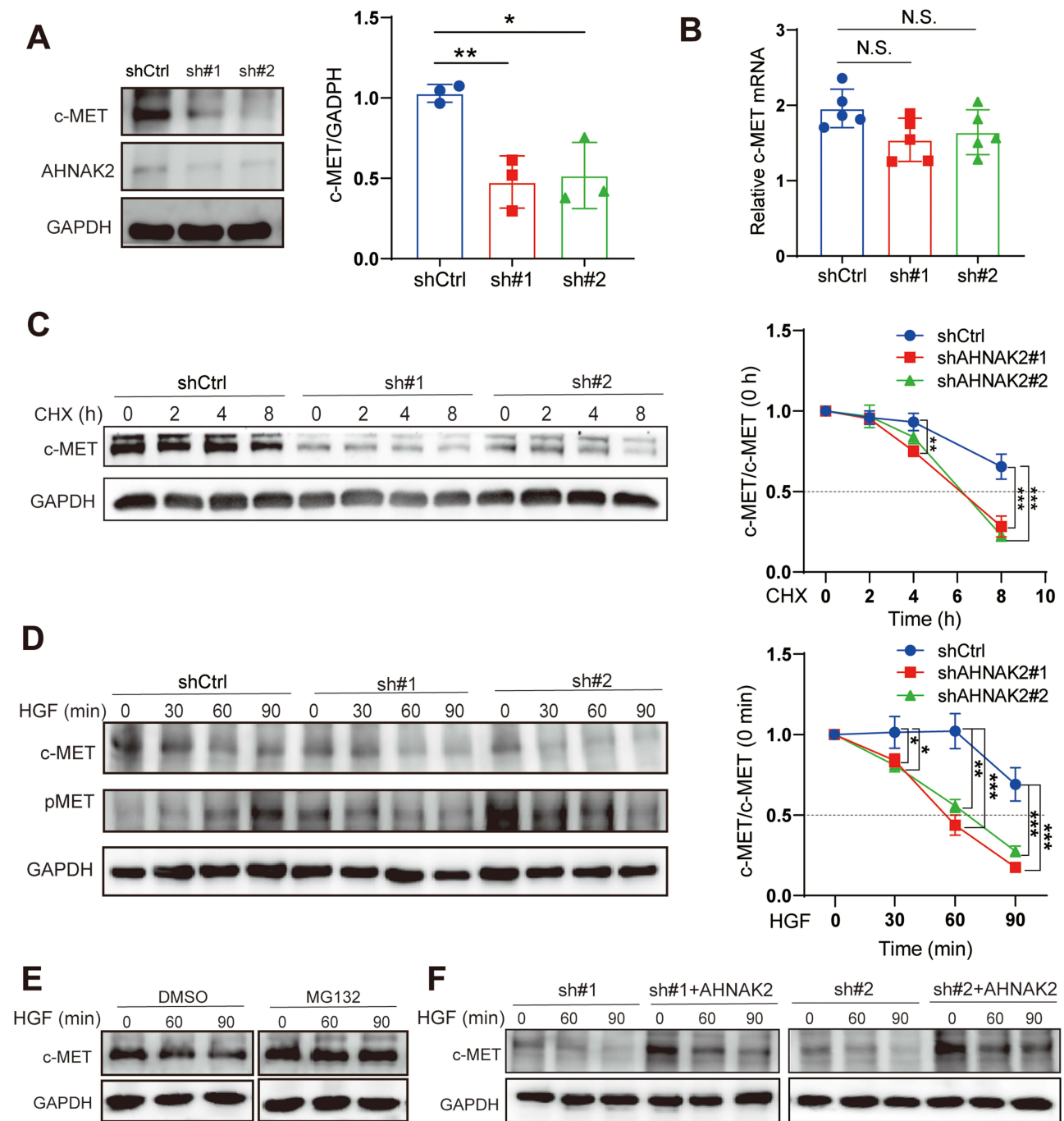
Figure 7 AHNAK2 stabilizes c-MET from degradation. (**A**) c-MET and AHNAK2 protein expression levels in PANC-1 cells of shAHNAK2 (n=3). (**B**) c-MET mRNA expression levels in PANC-1 cells of shControl and shAHNAK2 groups (n=5). (**C**) Representative Western blot images and degradation ratio curve of c-MET protein in shAHNAK2 PANC-1 cells after treated with cycloheximide at time gradients (n=3). (**D**) Representative Western blot images and time course of c-MET protein levels in shControl and shAHNAK2 PANC-1 cells in response to hepatocyte growth factor (HGF) stimulation (n=3). (**E**) HGF-induced c-MET accumulation in PANC-1 cells in the presence or absence of the proteasome inhibitor MG132 (n=3). (**F**) Rescue of AHNAK2 prevents c-MET from degradation. Representative Western blot image of c-MET levels in PANC-1 cells with shAHNAK2 or AHNAK2 re-expression. Each bar represents Mean ± SD. *p>0.05, **P>0.01; p***<0.001.
Abbreviation: N.S., not significant.

accumulation by inhibiting degradation. This suggested that AHNAK2 functions as a regulator of c-MET accumulation. Furthermore, inactivation of the HGF/c-MET signaling pathway may be attributed to the increased kinetics of c-MET degradation induced by AHNAK2 silencing.

The HGF/c-MET pathway has shown potential as an important therapeutic target for many solid tumors. Selectively or unselectively targeting TKIs, as well as monoclonal antibodies against c-MET, have been suggested as potential targeted treatments. However, the effectiveness and blocking efficiency of these approaches have been deemed unsatisfactory.[36] Thus, patients with PDAC may benefit from a combination strategy involving AHNAK2 inhibitors or antagonists. This approach offers an alternative mean of enhancing the effectiveness of TKIs by expediting the degradation of the c-MET receptor.

Conclusions

In conclusion, our results confirm the pivotal role of AHNAK2 in tumorigenesis and malignant progression of PDAC. The tumor-promoting effects driven by AHNAK2 are dependent on c-MET signaling, with AHNAK2 silencing leading to the inactivation of the HGF/c-MET pathway by compromising c-MET stability. These findings suggest the potential of targeting AHNAK2 as an innovative strategy to enhance the treatment efficacy for PDAC. In addition, to broaden the clinical applications of AHNAK2 in PDAC, the concrete mechanisms or targeted sequences through which AHNAK2 regulates the stability of c-MET need to be further validated.

Data Sharing Statement

The original data presented in this study are included in the article and its Supplementary Materials. Other supporting data are available from the corresponding author upon reasonable request.

Ethics Statement

The animal study was reviewed and approved by the Animal Experimental Research Ethics Committee of South China University of Technology (Ethics No.2022-059). The studies involving human participants were reviewed and approved by Ethics Committee of Sun Yat-sen Memorial Hospital (Ethics No. SYSKY-2023-735-01). The patients/participants provided their written informed consent to participate in this study.

Funding

Disclosure

The authors declare that they have no competing interests in this work.

References

1. Siegel RL, Miller KD, Wagle NS, Jemal A. Cancer statistics, 2023. *CA Cancer J Clin*. 2023;73(1):17–48. doi:10.3322/caac.21763
2. Huang J, Lok V, Ngai CH, et al. Worldwide burden of, risk factors for, and trends in pancreatic cancer. *Gastroenterology*. 2021;160(3):744–754. doi:10.1053/j.gastro.2020.10.007
3. Waddell N, Pajic M, Patch AM, et al. Whole genomes redefine the mutational landscape of pancreatic cancer. *Nature*. 2015;518(7540):495–501. doi:10.1038/nature14169
4. Li Petri G, Cascioferro SM, El Hassouni B, et al. Biological evaluation of the antiproliferative and anti-migratory activity of a series of 3-(6-Phenylimidazo[2,1- b][1,3,4]thiadiazol-2-yl)-1 H -indole derivatives against pancreatic cancer cells. *Anticancer Res*. 2019;39(7):3615–3620. doi:10.21873/anticanres.13509
5. Carbone D, De Franco M, Pecoraro C, et al. Discovery of the 3-Amino-1,2,4-triazine-based library as selective PDK1 inhibitors with therapeutic potential in highly aggressive pancreatic ductal adenocarcinoma. *Int J Mol Sci*. 2023;24(4):3679. doi:10.3390/ijms24043679
6. Duan H, Li L, He S. Advances and prospects in the treatment of pancreatic cancer. *Int J Nanomed*. 2023;18:3973–3988. doi:10.2147/IJN.S413496
7. Yang X-Y, Y-f L, J-x X, Du Y-Z, R-s Y. Recent Advances in Well-Designed Therapeutic Nanosystems for the Pancreatic Ductal Adenocarcinoma Treatment Dilemma. *Molecules*. 2023;28(3):1506. doi:10.3390/molecules28031506
8. Komuro A, Masuda Y, Kobayashi K, et al. The AHNAKs are a class of giant propeller-like proteins that associate with calcium channel proteins of cardiomyocytes and other cells. *Proc Natl Acad Sci USA*. 2004;101(12):4053–4058. doi:10.1073/pnas.0308619101
9. Zardab M, Stasinos K, Grose RP, Kocher HM. The obscure potential of AHNAK2. *Cancers*. 2022;14(3):528. doi:10.3390/cancers14030528
10. Wang M, Li X, Zhang J, et al. AHNAK2 is a novel prognostic marker and oncogenic protein for clear cell renal cell carcinoma. *Theranostics*. 2017;7(5):1100–1113. doi:10.7150/thno.18198

11. Ye R, Liu D, Guan H, et al. AHNAK2 promotes thyroid carcinoma progression by activating the NF-κB pathway. *Life Sci*. 2021;286:120032. doi:10.1016/j.lfs.2021.120032

12. Liu G, Guo Z, Zhang Q, Liu Z, Zhu D. AHNAK2 promotes migration, invasion, and epithelial-mesenchymal transition in lung adenocarcinoma cells via the TGF-β/Smad3 pathway. *Onco Targets Ther*. 2020;13:12893–12903. doi:10.2147/OTT.S281517

13. Li M, Liu Y, Meng Y, Zhu Y. AHNAK nucleoprotein 2 performs a promoting role in the proliferation and migration of uveal melanoma cells. *Cancer Biother Radiopharm*. 2019;34(10):626–633. doi:10.1089/cbr.2019.2778

14. Almeida PP, Cardoso CP, de Freitas LM. PDAC-ANN: an artificial neural network to predict pancreatic ductal adenocarcinoma based on gene expression. *BMC Cancer*. 2020;20(1):82. doi:10.1186/s12885-020-6533-0

15. Yang ZQ, Liu YJ, Zhou XL. An integrated microarray analysis reveals significant diagnostic and prognostic biomarkers in pancreatic cancer. *Med Sci Monit*. 2020;26:e921769. doi:10.12659/MSM.921769

16. Huang J, Zhou Y, Zhang H, Wu Y. A neural network model to screen feature genes for pancreatic cancer. *BMC Bioinf*. 2023;24(1):193. doi:10.1186/s12859-023-05322-z

17. Comoglio PM, Trusolino L, Boccaccio C. Known and novel roles of the MET oncogene in cancer: a coherent approach to targeted therapy. *Nat Rev Cancer*. 2018;18(6):341–358. doi:10.1038/s41568-018-0002-y

18. Modica C, Tortarolo D, Comoglio PM, Basilico C, Vigna E. MET/HGF co-targeting in pancreatic cancer: a tool to provide insight into the tumor/stroma crosstalk. *Int J Mol Sci*. 2018;19(12):3920. doi:10.3390/ijms19123920

19. Jones S, Zhang X, Parsons DW, et al. Core signaling pathways in human pancreatic cancers revealed by global genomic analyses. *Science*. 2008;321(5897):1801–1806. doi:10.1126/science.1164368

20. Jin H, Yang R, Zheng Z, et al. MetMAb, the one-armed 5D5 anti-c-Met antibody, inhibits orthotopic pancreatic tumor growth and improves survival. *Cancer Res*. 2008;68(11):4360–4368. doi:10.1158/0008-5472.CAN-07-5960

21. Yu J, Ohuchida K, Mizumoto K, et al. Overexpression of c-met in the early stage of pancreatic carcinogenesis; altered expression is not sufficient for progression from chronic pancreatitis to pancreatic cancer. *World J Gastroenterol*. 2006;12(24):3878–3882. doi:10.3748/wjg.v12.i24.3878

22. Delitto D, Vertes-George E, Hughes SJ, Behrns KE, Trevino JG. c-Met signaling in the development of tumorigenesis and chemoresistance: potential applications in pancreatic cancer. *World J Gastroenterol*. 2014;20(26):8458–8470. doi:10.3748/wjg.v20.i26.8458

23. Wang DW, Zheng HZ, Cha N, et al. Down-regulation of AHNAK2 inhibits cell proliferation, migration and invasion through inactivating the MAPK pathway in lung adenocarcinoma. *Technol Cancer Res Treat*. 2020;19:1533033820957006. doi:10.1177/1533033820957006

24. Lu Y, Xu D, Peng J, et al. HNF1A inhibition induces the resistance of pancreatic cancer cells to gemcitabine by targeting ABCB1. *EBioMedicine*. 2019;44:403–418. doi:10.1016/j.ebiom.2019.05.013

25. Lakshmanan I, Marimuthu S, Chaudhary S, et al. Muc16 depletion diminishes KRAS-induced tumorigenesis and metastasis by altering tumor microenvironment factors in pancreatic ductal adenocarcinoma. *Oncogene*. 2022;41(48):5147–5159. doi:10.1038/s41388-022-02493-6

26. Hingorani SR, Wang L, Multani AS, et al. Trp53R172H and KrasG12D cooperate to promote chromosomal instability and widely metastatic pancreatic ductal adenocarcinoma in mice. *Cancer Cell*. 2005;7(5):469–483. doi:10.1016/j.ccr.2005.04.023

27. Wood LD, Canto MI, Jaffee EM, Simeone DM. Pancreatic cancer: pathogenesis, screening, diagnosis, and treatment. *Gastroenterology*. 2022;163(2):386–402.e381. doi:10.1053/j.gastro.2022.03.056

28. Gherardi E, Sandin S, Petoukhov MV, et al. Structural basis of hepatocyte growth factor/scatter factor and MET signalling. *Proc Natl Acad Sci USA*. 2006;103(11):4046–4051. doi:10.1073/pnas.0509040103

29. Moosavi F, Giovannetti E, Saso L, Firuzi O. HGF/MET pathway aberrations as diagnostic, prognostic, and predictive biomarkers in human cancers. *Crit Rev Clin Lab Sci*. 2019;56(8):533–566. doi:10.1080/10408363.2019.1653821

30. Xu R, Liu X, Li A, et al. c-Met up-regulates the expression of PD-L1 through MAPK/NF-κBp65 pathway. *J Mol Med*. 2022;100(4):585–598. doi:10.1007/s00109-022-02179-2

31. Yu J, Zhang L, Peng J, et al. Dictamnine, a novel c-Met inhibitor, suppresses the proliferation of lung cancer cells by downregulating the PI3K/AKT/mTOR and MAPK signaling pathways. *Biochem Pharmacol*. 2022;195:114864. doi:10.1016/j.bcp.2021.114864

32. Zhang Y, Xia M, Jin K, et al. Function of the c-Met receptor tyrosine kinase in carcinogenesis and associated therapeutic opportunities. *Mol Cancer*. 2018;17(1):45. doi:10.1186/s12943-018-0796-y

33. Li C, Wu JJ, Hynes M, et al. c-Met is a marker of pancreatic cancer stem cells and therapeutic target. *Gastroenterology*. 2011;141(6):2218–2227.e2215. doi:10.1053/j.gastro.2011.08.009

34. Pothula SP, Xu Z, Goldstein D, Pirola RC, Wilson JS, Apte MV. Targeting HGF/c-MET axis in pancreatic cancer. *Int J Mol Sci*. 2020;21(23):9170. doi:10.3390/ijms21239170

35. Luna J, Boni J, Cuatrecasas M, et al. DYRK1A modulates c-MET in pancreatic ductal adenocarcinoma to drive tumour growth. *Gut*. 2019;68(8):1465–1476. doi:10.1136/gutjnl-2018-316128

36. Bradley CA, Salto-Tellez M, Laurent-Puig P, et al. Targeting c-MET in gastrointestinal tumours: rationale, opportunities and challenges. *Nat Rev Clin Oncol*. 2017;14(9):562–576. doi:10.1038/nrclinonc.2017.40